ARMY RESEARCH LABORATORY

Ab Initio and Nonlocal Density Functional Study of 1,3,5-trinitro-s-triazine (RDX) Conformers

by Betsy M. Rice
and Cary F. Chabalowski

ARL-TR-1586

January 1998

Army Research Laboratory
Aberdeen Proving Ground, MD 21005-5066

ARL-TR-1586 **January 1998**

Ab Initio and Nonlocal Density Functional Study of 1,3,5-trinitro-s-triazine (RDX) Conformers

Betsy M. Rice, Cary F. Chabalowski
Weapons and Materials Research Directorate, ARL

Abstract

Geometry optimizations and normal-mode analyses of three conformers of 1,3,5-trinitro-s-triazine (RDX) are performed using second-order Moller-Plesset (MP2) and nonlocal density functional theory (DFT) methods. The density function used in this study is B3LYP. The three conformers of RDX are distinguished mainly by the arrangement of the nitro groups relative to the ring atoms of the RDX molecule. NO_2 groups arranged in either pseudo-equatorial or axial positions are denoted with (E) or (A), respectively. The axial-axial-equitorial (AAE) conformer has C_s symmetry and is the structure in the room-temperature-stable crystal (α-RDX). The axial-axial-axial (AAA) and equitorial-equitorial-equitorial (EEE) conformers have C_{3v} symmetry, a symmetry consistent with vapor and β-solid infrared (IR) spectra. The AAE and AAA conformers are studied at the MP2/6-31G*, B3LYP/6-31G*, and B3LYP/6-311+G** levels, and the EEE conformer is studied using the B3LYP density function and the 6-31G* and 6-311+G** basis sets. The geometric parameters and IR spectra of the AAA conformer are in good agreement with experimental gas-phase and β-solid data, supporting the hypotheses derived from experiment that the AAA structure is the most probable conformer in vapor-phase and β-solid RDX. The B3LYP/ 6-311+G** structures and simulated IR spectra are in closest agreement with experimental data. The MP2/6-31G* structures and spectra are in poorest agreement with experiment.

Acknowledgments

All calculations were performed on the Silicone Graphics, Inc., (SGI) Power Challenge Array at the Department of Defense (DOD) High-Performance Computing Site at the U.S. Army Research Laboratory (ARL), Aberdeen Proving Ground (APG), MD.

INTENTIONALLY LEFT BLANK.

Table of Contents

INTENTIONALLY LEFT BLANK.

List of Figures

List of Tables

INTENTIONALLY LEFT BLANK.

1. Introduction

Advances in the development of nonlocal density functional theory (DFT) [1–5] and in computer architectures have allowed for reliable electronic-structure investigations of large polyatomic molecules. We have subjected the well-studied explosive, 1,3,5-trinitro-s-triazine, commonly known as RDX, to both DFT and *ab initio* treatments. The results presented here provide atomic-level information about RDX conformers, as well as indicate the suitability of current theoretical treatments to systems such as these. In this work, we determine the geometries of three conformers of RDX and characterize them through normal-mode analyses using electronic-structure methods. Comparisons of structural parameters, vibrational frequencies, and simulated infrared (IR) spectra against measured properties are given.

There have been attempts at treating RDX with electronic-structure and semi-empirical theories [6–7]; however, the highest level of theory used for geometry optimizations reported in these studies is the SCF-MO (Hartree-Fock [HF]) level using basis sets ranging from STO-3G to 4-21G [6–7]. These levels of calculations can provide a crude approximation to optimized structures; however, known deficiencies in the theory beg for further theoretical treatments to provide a reliable prediction of the system. An example resulting from the deficiencies in the HF theory is seen in the SCF/4-21G calculations of Coffin et al. [7], in which SCF geometry optimizations were attempted for four conformers of RDX. The four conformers of RDX differ mainly in the position of the nitro groups relative to the ring atoms. The ring atoms are arranged in the chair conformation. The conformers were labeled according to axial (A) or pseudo-equatorial positioning (E) of the nitro groups about the ring. We adopt the same nomenclature for the conformers in this work. All nitro groups of the axial-axial-axial (AAA) conformer occupy axial positions, and all nitro groups of the equitorial-equitorial-equitorial (EEE) conformer occupy pseudo-equatorial positions. Both of these conformers belong to the C_{3v} point group. Two nitro groups occupy axial positions on the axial-axial-equitorial (AAE) conformer and the remaining nitro group is in the pseudo-equatorial position. For the AEE conformer, two nitro groups occupy pseudo-equatorial positions, and the remaining nitro group is axial [7]. The AAE and AEE conformers belong to the C_s point group. Figure 1 illustrates all of

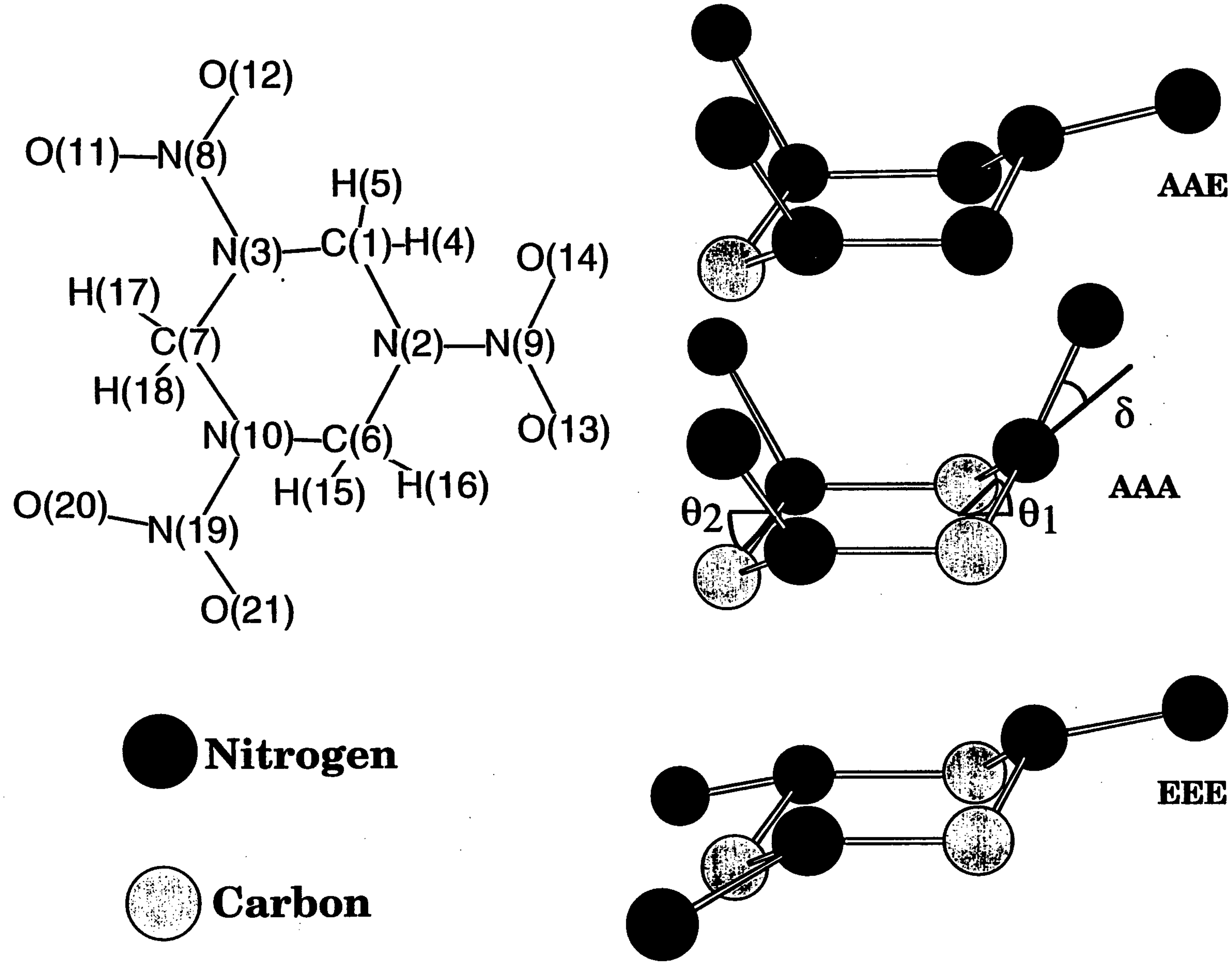

Figure 1. Structures of the AAE, AAA, and EEE Conformers of RDX. Atom Labels on the Two-Dimensional Projection of the RDX Molecule Are Consistent With the Internal Coordinates in Tables 1 and 2. For Clarity, the Hydrogen and Oxygen Atoms Are Not Illustrated in the Three-Dimensional Representations.

these conformers, except for the AEE species. For clarity, we have not shown the hydrogen atoms or the oxygen atoms of the nitro groups for the AAA, EEE, and AAE conformers in this figure. Normal-mode analyses for each of the SCF/4-21G optimized structures indicated that only the AAA conformer had all real vibrational frequencies and was therefore the only stable species predicted at this level of theory. The remaining conformers, each of which had at least one equatorial nitro group, had imaginary frequencies, indicating they were not stable structures. Neutron diffraction measurements of solid α-RDX (the form that is stable at room temperature) provided the crystal structure and atomic arrangements of the molecules in the crystal [8]. The molecular geometry of α-RDX is consistent with the AAE conformer. This indicates that either the SCF/4-21G level of theory is not sufficient to correctly describe this conformer, or that the crystal field stabilizes the AAE conformer in the α-solid. A second crystalline form of RDX exists (β-RDX), but it is extremely unstable, and no direct experimental structural information is available for this form [9]. Karpowicz and Brill [9] recorded the IR spectra of both α- and β-RDX, as well as RDX in the vapor phase. The IR spectra of α- and β-RDX have distinct differences, and the fewer modes in the β-solid suggest a higher molecular symmetry than that of α-RDX. Additionally, the β-solid spectrum has features that are similar to vapor-phase RDX [9]. Karpowicz and Brill concluded that the molecular conformation of the RDX in the β-solid and in the vapor phase has a molecular symmetry of C_{3v} and suggested two possible structures with this symmetry [9]. One structure has the nitro groups occupying all axial positions (AAA), and one has the nitro groups occupying all pseudo-equatorial positions (EEE). The measurements did not provide sufficient information to distinguish between the two possibilities. Subsequent electron diffraction experiments indicated that the AAA RDX conformer is consistent with the diffraction patterns, and structural parameters were obtained from fitting models to the experimental data [10].

We compare *ab initio* and nonlocal DFT predictions of structural parameters and vibrational frequencies for the AAE, AAA, and EEE conformers of RDX against the experimental information [8–10]. Second-order Moeller-Plesset (MP2) [11] geometry optimizations using the 6-31G* basis set [12–14] are used to locate the AAE and AAA conformers. Nonlocal DFT geometry optimizations using the 6-31G* [12–14] and 6-311+G** [15–16] basis sets and the B3LYP density functional [17–19] are performed for the same conformers and compared against MP2 to determine the magnitude of difference in theoretical treatments. As shown hereafter, the better agreement of the B3LYP/6-311+G** predictions with experiment strongly suggests that this level is sufficient to accurately determine stable structures for the RDX conformers. Normal-mode analyses are used to characterize each stable point, and IR vibrational spectra are simulated for comparison with experiment. The spectra are simulated by fitting the predicted IR intensities to Lorentzian functions with bandwidths arbitrarily set to 8. All calculations are performed using the Gaussian 94 set of quantum chemistry programs [20]. All geometry optimizations meet or exceed the default convergence criteria assigned by Gaussian 94 [20]. The DFT calculations use the default grid size given in Gaussian 94 [20].

2. Results and Discussion

2.1 AAE Structural Data. Table 1 lists the geometric parameters of the AAE conformer predicted with various theoretical methods and provides a comparison with parameters obtained from neutron diffraction measurements of α-RDX [8]. The labeling of the atoms in the two-dimensional projection of the RDX molecule in Figure 1 is consistent with the labeling of the internal coordinates in Table 1. The angle θ_1 shown for the AAA conformer in Figure 1 is the angle between the C(1)-N(2)-C(6) plane and the plane containing the C(1)-N(3)-N(10)-C(6) atoms. Angle θ_2 denotes the angle between the planes containing the N(3)-C(7)-N(10) atoms and the C(1)-N(3)-N(10)-C(6) atoms, respectively. The angle δ is the angle between the plane of the C(1)-N(2)-C(6) atoms and the N(2)-N(9) bond. Of the three theoretical treatments, the B3LYP/6-311+G** predictions have the smallest overall deviation from experiment for the bonds and bond angles, and the MP2/6-31G* has the largest overall deviation from experiment. The largest differences between theoretical predictions at the three levels presented here, and the experimental determinations are in the N-N bond lengths and the C-N-N angles. All of the theoretical predictions overestimate the N-N bond lengths by ~2.5–4.5%, and the MP2/6-31G* calculations overestimate the N-O bond lengths by 2.1–2.6%. All theoretical methods also overestimate the C(1)-H(4) bond by ~4%. The B3LYP/6-311+G** predictions of the remaining bonds are in closest overall agreement with experiment. All of the theoretical methods underestimate the C-N(2)-N bond angles by ~3.5–6.0%. The

Table 1. Structural Parameters of the AAE RDX Conformer

Bond (Å)	MP2/6-31G*	B3LYP/6-31G*	B3LYP/6-311+G**	Experiment [8]
C(1)-N(2)	1.4700	1.4733	1.4748	1.464
C(1)-N(3)	1.4484	1.449	1.4488	1.443
C(7)-N(3)	1.4618	1.4621	1.4628	1.468
C(7)-N(10)	1.4618	1.4621	1.4628	1.458
C(6)-N(10)	1.4484	1.449	1.4488	1.440
C(6)-N(2)	1.4700	1.4733	1.4748	1.450
C(1)-H(4)	1.1001	1.0994	1.0974	1.058
C(1)-H(5)	1.0846	1.0841	1.0827	1.092
C(7)-H(17)	1.0864	1.0851	1.0839	1.085
C(7)-H(18)	1.0936	1.0938	1.0918	1.087
C(6)-H(15)	1.1001	1.0994	1.0974	1.088
C(6)-H(16)	1.0846	1.0841	1.0827	1.075
N(2)-N(9)	1.4105	1.4022	1.4051	1.351
N(3)-N(8)	1.4370	1.4317	1.4335	1.392
N(10)-N(19)	1.4360	1.4317	1.4334	1.398
N(9)-O(13)	1.236	1.2258	1.2195	1.209
N(9)-O(14)	1.236	1.2258	1.2195	1.233
N(8)-O(11)	1.2319	1.2202	1.2137	1.203
N(8)-O(12)	1.2324	1.2211	1.2148	1.207
N(19)-O(20)	1.2319	1.2202	1.2137	1.201
N(19)-O(21)	1.2324	1.2211	1.2148	1.205

Angle (°)	MP2/6-31G*	B3LYP/6-31G*	B3LYP/6-311+G**	Experiment
θ_1	54.14	50.05	50.87	53.31
θ_2	42.74	41.44	41.44	43.73
δ	−27.91	−24.39	−24.08	−12.59

Table 1. Structural Parameters of the AAE RDX Conformer (continued)

Angle (°)	MP2/6-31G*	B3LYP/6-31G*	B3LYP/6-311+G**	Experiment
N(2)-C(1)-N(3)	108.84	109.26	109.09	107.8
N(2)-C(1)-H(4)	111.36	110.90	110.64	109.9
N(2)-C(1)-H(5)	109.61	109.38	109.57	110.0
N(3)-C(1)-H(4)	106.90	107.55	107.49	108.0
N(3)-C(1)-H(5)	110.19	109.95	110.30	110.0
H(4)-C(1)-H(5)	109.89	109.78	109.73	111.0
N(3)-C(2)-N(10)	113.38	112.71	112.45	111.7
N(3)-C(2)-H(17)	109.91	109.76	109.99	110.1
N(3)-C(2)-H(18)	106.80	107.21	107.24	106.9
N(10)-C(2)-H(17)	109.91	109.76	109.99	110.7
N(10)-C(2)-H(18)	106.80	107.22	107.24	107.2
H(17)-C(2)-H(18)	109.93	110.09	109.84	110.1
N(10)-C(6)-N(2)	108.84	109.26	109.09	108.4
N(10)-C(6)-H(15)	106.90	107.55	107.49	107.4
N(10)-C(6)-H(16)	110.19	109.95	110.30	111.1
N(2)-C(6)-H(15)	111.36	110.90	110.64	109.6
N(2)-C(6)-H(16)	109.61	109.38	109.57	111.3
H(15)-C(6)-H(16)	109.89	109.78	109.73	108.8
C(6)-N(2)-C(1)	112.76	115.03	114.52	115.1
C(6)-N(2)-N(9)	113.65	115.09	115.42	120.9
C(1)-N(2)-N(9)	113.65	115.09	115.42	119.7
N(2)-N(9)-O(13)	116.52	116.60	116.64	117.2
N(2)-N(9)-O(14)	116.52	116.60	116.64	117.8
O(13)-N(9)-O(14)	126.91	126.78	126.68	125.0
C(1)-N(3)-C(7)	113.88	115.47	115.52	114.6
C(1)-N(3)-N(8)	113.83	116.05	116.43	117.1
C(7)-N(3)-N(8)	114.46	116.51	116.91	116.6
N(3)-N(8)-O(11)	115.78	116.11	116.10	117.2

Table 1. Structural Parameters of the AAE RDX Conformer (continued)

Angle (°)	MP2/6-31G*	B3LYP/6-31G*	B3LYP/6-311+G**	Experiment
N(3)-N(8)-O(12)	116.66	116.63	116.65	116.8
O(11)-N(8)-O(12)	127.37	127.11	127.11	125.7
C(7)-N(10)-C(6)	113.88	115.47	115.52	114.8
C(7)-N(10)-N(19)	114.46	116.51	116.91	117.5
C(6)-N(10)-N(19)	113.83	116.05	116.43	115.6
N(10)-N(19)-O(20)	115.78	116.11	116.10	117.3
N(10)-N(19)-O(21)	116.66	116.63	116.65	117.0
O(20)-N(19)-O(21)	127.37	127.11	127.11	125.5

MP2/6-31-G* predictions of the remaining C-N-N bonds underestimate the values by 1.5–2.8%, while the B3LYP predictions are within 1% of experiment. The predicted angles θ_1 and θ_2, which are indicative of the deviation of the ring atoms from planarity, are within 3.1 and 2.4% or less, respectively, from the experimental values. The theoretical predictions of δ (which measures the tilt of the N-N bond away from the CNC plane) disagree with experiment by 11.5° to 15.3° and could be due to crystal-field effects. The B3LYP/6-311+G** prediction of δ is in closest agreement with experiment. The overall good agreement in the geometries is remarkable, since the neutron diffraction information was determined from molecules in the crystal state, and the theoretical calculations involve a single RDX molecule. The crystal field does not significantly distort the molecule from C_s symmetry.

2.2 AAA and EEE Structural Data. The AAA and EEE conformers suggested as possible structures for RDX in the vapor and β-solid phases both have C_{3v} symmetry [9]. Theoretical predictions of geometric parameters for both conformers are given in Table 2, along with the experimental information for vapor-phase RDX. In this table, the individual geometric parameters are given along with the averages of symmetry equivalent parameters. The averages are compared against the experimental numbers. The theoretical predictions of the bond lengths for both conformers at all levels are within 1% of the experimental result. The agreement of bond angles with

Table 2. Structural Parameters of the AAA and EEE RDX Conformers

	AAA			EEE		Expt.
	MP2	B3LYP		B3LYP		
	6-31G*	6-31G*	6-311+G**	6-31G*	6-311+G**	
CN						
C(1)-N(2)	1.4586	1.4603	1.4607	1.4612	1.4612	
C(6)-N(2)	1.4586	1.4601	1.4608	1.4606	1.4612	
C(6)-N(10)	1.4586	1.4604	1.4607	1.4596	1.4604	
C(7)-N(10)	1.4586	1.4599	1.4605	1.4604	1.4605	
C(7)-N(3)	1.4586	1.4606	1.4607	1.4575	1.4593	
C(1)-N(3)	1.4586	1.4606	1.4605	1.4577	1.4598	
<CN>	1.4586	1.4603	1.4607	1.4595	1.4604	1.464
NN						
N(2)-N(9)	1.4280	1.4230	1.4237	1.4011	1.4043	
N(10)-N(19)	1.4280	1.4223	1.4236	1.4010	1.4041	
N(3)-N(8)	1.4280	1.4223	1.4229	1.3987	1.4030	
<NN>	1.4280	1.4225	1.4234	1.4003	1.4038	1.413
NO						
N(8)-O(11)	1.2331	1.2219	1.2157	1.2254	1.2189	
N(8)-O(12)	1.2331	1.2221	1.2156	1.2255	1.2189	
N(9)-O(13)	1.2331	1.2219	1.2155	1.2251	1.2187	
N(9)-O(14)	1.2331	1.2218	1.2156	1.2252	1.2188	
N(19)-O(20)	1.2331	1.2219	1.2157	1.2252	1.2188	
N(19)-O(21)	1.2331	1.2222	1.2156	1.2252	1.2187	
<NO>	1.2331	1.2220	1.2156	1.2253	1.2188	1.213

Note: Bond lengths in angstroms and angles in degrees.

Table 2. Structural Parameters of the AAA and EEE RDX Conformers (continued)

	AAA			EEE		Expt.
	MP2	B3LYP		B3LYP		
	6-31G*	6-31G*	6-311+G**	6-31G*	6-311+G**	
CH						
C(1)-H(4)	1.0947	1.0947	1.0929	1.1041	1.1022	
C(6)-H(15)	1.0947	1.0947	1.0928	1.1043	1.1023	
C(7)-H(18)	1.0947	1.0948	1.0928	1.1043	1.1022	
C(1)-H(5)	1.0866	1.0854	1.0843	1.0846	1.0830	
C(6)-H(16)	1.0866	1.0854	1.0843	1.0844	1.0828	
C(7)-H(17)	1.0857	1.0856	1.0843	1.0845	1.0829	
<CH>	1.0905	1.0901	1.0886	1.0944	1.09269	1.089
NCN						
N(2)-C(6)-N(10)	113.64	112.71	112.47	106.07	105.92	
N(2)-C(1)-N(3)	113.64	112.79	112.43	105.97	105.82	
N(3)-C(7)-N(10)	113.64	112.72	112.46	105.92	105.73	
<NCN>	113.64	112.74	112.45	105.99	105.82	109.4
CNC						
C(1)-N(2)-C(6)	114.08	115.50	115.68	117.62	116.95	
C(6)-N(10)-C(7)	114.08	115.67	115.72	117.44	116.90	
C(1)-N(3)-C(7)	114.08	115.62	115.80	117.88	117.12	
<CNC>	114.08	115.60	115.73	117.65	116.99	123.7
CNN						
C(1)-N(2)-N(9)	116.08	117.45	117.94	115.13	115.56	
C(1)-N(3)-N(8)	116.07	117.43	118.10	115.89	116.01	
C(6)-N(2)-N(9)	116.08	117.40	117.94	115.09	115.53	
C(6)-N(10)-N(19)	116.08	117.46	117.99	115.31	115.69	

Note: Bond lengths in angstroms and angles in degrees.

Table 2. Structural Parameters of the AAA and EEE RDX Conformers (continued)

	AAA			EEE		Expt.
	MP2	B3LYP		B3LYP		
	6-31G*	6-31G*	6-311+G**	6-31G*	6-311+G**	
C(7)-N(10)-N(19)	116.08	117.51	118.00	115.31	115.72	
C(7)-N(3)-N(8)	116.08	117.48	118.10	115.93	116.01	
<CNN>	116.08	117.46	118.01	115.44	115.75	116.3
ONO						
O(11)-N(8)-O(12)	127.24	127.00	126.97	126.95	126.83	
O(13)-N(9)-O(14)	127.24	127.04	126.98	126.98	126.84	
O(20)-N(19)-O(21)	127.24	127.00	126.99	126.98	126.85	
<ONO>	127.24	127.01	126.98	126.97	126.84	125.5
HCH						
H(4)-C(1)-H(5)	109.89	110.09	109.79	109.39	109.56	
H(17)-C(7)-H(18)	109.89	110.02	109.81	109.41	109.59	
H(15)-C(6)-H(16)	109.89	110.09	109.79	109.37	109.55	
<HCH>	109.89	110.07	109.80	109.39	109.57	105.1
ϕ	-0.03	-0.01	-0.07	-0.01	0.07	19.1
θ_1	42.25	41.75	42.09	51.36	52.45	33.9
θ_2	42.07	40.48	40.65	45.80	47.00	
δ	23.37	19.70	18.41	-21.01	-21.38	19.9
γ	346.24	350.50	351.75	348.54	348.56	356.3

Note: Bond lengths in angstroms and angles in degrees.

experiment, however, is not as good for the C_{3v} conformers as it was for the AAE structure. The largest disagreement between the calculated and experimental values is in the CNC angles. The B3LYP/ 6-311+G** predictions for AAA and EEE are 115.7° and 117.0°, respectively, which underestimate the experimental value of 123.7° by 8.0° to 6.7°. The agreement of the MP2/6-31G* AAA prediction of this angle with experiment is even worse (~10°). It is notable that the theoretical predictions of the CNC angle for these conformers are closer to the experimental value for the AAE conformer (~114.8°). Shiskov et al. [10] note a large change in the CNC angles between the gas phase and α-solid AAE conformers, but attribute the difference to crystal-field effects for the AAE conformer. As previously mentioned, this is not supported by the current results where theory (for the isolated AAE molecule) predicts an AAE structure in close agreement with the experimental crystal structure. In addition, the theoretical predictions for the CNC angles are quite similar for all three conformers and agree with the experimental AAE crystal CNC angle to within 2.8° or less. Theoretical predictions of the angle θ_1 are greater than experiment by ~8° and ~18° for the AAA and EEE conformers, respectively. These indicate that experiment predicts ring structures closer to planarity than either of the theoretical C_{3v} structures, although the AAA values are closer to experiment than the EEE. We have also included the predicted values for γ, which are included in the experimental paper and defined as the sum of the three bond angles involving the ring nitrogen atom. This value reflects the degree to which the ring nitrogen is coplanar with its three attached neighbors. This parameter for both conformers at all levels is in close agreement with experiment.

The geometric parameter ϕ, defined by Shishkov et al. [10] as the torsional angle about the N-N bond, was reported to be 19.1°. The value for the optimized structures calculated at all levels in this study is 0°, indicating a geometry in which the "C. . .C and O. . .O lines of the C_2N-NO_2 fragment are coplanar" [6]. A geometry optimization of the AAA conformer at the B3LYP/6-31G* level was attempted in which the starting geometry had the angle ϕ set to 19.3°. The value of the angle ϕ in the resulting optimized structure was 0°, and the remaining geometric parameters are equal to those given in Table 2. The discrepancy between theory and experiment could be related to the fitting procedure used in the experimental analysis. In the experimental analysis, structural models were assumed, each of which was described by a set of variables that would be parameterized to provide best agreement with the electron diffraction measurements. Three assumptions were made about structural relationships that were held fixed throughout the fitting procedures: the CH_2 moieties have local C_{2v} symmetry, the CNN angles within a molecule are equal, and the NO_2 geometry is planar. The final geometry was obtained by an iterative fitting procedure in which one parameter was optimized at a time when the remaining parameters were held fixed. Initially, all parameters were assigned starting values taken from the literature for similar compounds. After the iterative parameter refinement, a final simultaneous least-squares fit of the parameter set was performed, resulting in the reported values. Such an iterative procedure could be subject to convergence to a local minimum in the parameter space. This is a possible explanation for the difference between the theoretical and experimental value of ϕ.

The information gained by the bond lengths and angles does not provide sufficient information to distinguish between the C_{3v} conformers, nor do the angles ϕ_1 and ϕ_2. However, the predicted values of δ for AAA are almost in exact agreement with the experimental value, while the EEE predictions are off by 41°. Therefore, based primarily on δ and less so on θ_1, the theoretical calculations clearly support the conclusions obtained from the experiment [10]; namely, that the vapor-phase structure of RDX is consistent with the nitro-group arrangement in the AAA conformer.

2.3 Vibrational Spectra. Harmonic vibrational frequencies for the three conformers were determined through normal-mode analyses; each conformer had six 0 frequencies, and the remaining frequencies were real, in contrast to the SCF/4-21G results [7]. Table 3 provides the calculated harmonic vibrational frequencies at the MP2/6-31G* and B3LYP/6-311+G** levels, corresponding IR intensities (in esu^2-cm^2) and symmetry assignments for each mode for comparison with the experimental assignments. Assignments identifying the nature of the vibrational modes are given in Table 4. The symmetry assignments correspond to the B3LYP/ 6-311+G** results, which appear to give the best reproduction of the experimental spectra, as shown hereafter. It is hoped that these assignments will be of help to experimentalists in interpreting observed spectra.

Simulated spectra based upon B3LYP/6-311+G** IR intensities and frequencies for the three conformers are compared against experimental IR spectra in Figure 2. The vibrational frequencies in this figure have been reduced by 3%.

It is clear that the simulated IR spectrum for the AAA conformer has several features that are similar to the experimental vapor and β-solid phase IR spectra in the mid-infrared (IR) region, particularly between 1,100 cm^{-1} and 1,650 cm^{-1} [9]. The theoretical IR spectrum between 1,100 and 1,500 cm^{-1} for the EEE conformer shows a band pattern in much poorer agreement with the

Table 3. Theoretical and Experimental Vibrational Frequencies of RDX Conformers

	AAE Conformer								AAA Conformer							EEE Conformer		
	Theoretical AAE					α-solid			Theoretical AAA					Vapor	β-solid	Theoretical EEE		
	MP2/6-31G		B3LYP/6-311+G**			Ref. [9]	Ref. [21]		MP2/6-31		B3LYP/6-311+G**			Ref. [9]	Ref. [9]	B3LYP/6-311+G**		
υ	Freq.	Int.	Freq.	Int.	Irr. Rep.	IR	IR	Raman	Freq.	Int.	Freq.	Int.	Irr. Rep.	IR	IR	Freq.	Int.	Irr. Rep.
1	3,277	8	3,206	10	A	3,074 w	3,075 s	3,075 m	3,265	9	3,194	17	A_1	3,065 vw	3,075 w	3,203	2	A_1
2	3,277	13	3,205	18	A′				3,265	11	3,192	18	E			3,200	23	E
3	3,272	13	3,199	17	A	3,065 w	3,066 s	3,067 m	3,265	11	3,192	17	E		3,067 w	3,199	22	E
4	3,155	11	3,081	16	A	3,001 w	3,001 m	3,001 s	3,144	28	3,070	50	A_1		3,005 w	2,964	117	A_1
5	3,083	2	3,016	51	A		2,948 w	2,949 m	3,138	0	3,064	1	E			2,959	6	E
6	3,083	41	3,015	4	A′				3,138	0	3,064	1	E			2,958	7	E
7	1,842	374	1,668	117	A	1,592 s	1,598 vs	1,593 w	1,836	158	1,658	1,123	E	1,584 vs	1,588 s,sh	1,637	126	E
8	1,837	97	1,648	654	A′	1,576 s	1,573 vs	1,570 w	1,836	158	1,658	1,122	E			1,637	126	E
9	1,816	276	1,623	504	A′	1,539 m	1,540 vs	1,538 w	1,828	0	1,627	0	A_2		1,458 w	1,619	0	A_2
10	1,547	127	1,496	135	A	1,533 m	1,532 s	1,508 vw	1,530	89	1,482	220	A_1	1,444 m	1,441 m,b	1,522	11	A_1
11	1,529	11	1,480	15	A′	1,458 m	1,459 s	1,456 w	1,508	26	1,466	86	E	1,420 m	1,419 m	1,510	19	E
12	1,518	116	1,468	123	A	1,436 m	1,434 m	1,433 w	1,508	27	1,464	84	E			1,509	19	E
13	1,445	124	1,420	206	A	1,423 m	1,423 m	1,422 sh	1,420	8	1,403	59	E	1,374 m	1,383 w	1,431	105	E
14	1,420	5	1,406	19	A′	1,388 m	1,389 s	1,387 w	1,420	8	1,402	56	E			1,430	109	E
15	1,395	1	1,374	6	A′		1,377	1,377 w	1,407	0	1,384	3	E			1,366	0	A_2
16	1,382	129	1,362	8	A′	1,351 m	1,352 m	1,346 w	1,407	0	1,381	10	E			1,350	48	A_1
17	1,376	0	1,362	172	A	1,311 m	1,310 s	1,309 s	1,373	0	1,363	1	A_2			1,336	85	E

Notes: vs - very strong, s - strong, m - medium, b - broad, sh - shoulder.
Frequencies and corresponding IR intensities are in cm^{-1} and esu^2-cm^2, respectively.
Symmetry assignments correspond to the B3LYP/6-311+G** results only.

Table 3. Theoretical and Experimental Vibrational Frequencies of RDX Conformers (continued)

	AAE Conformer								AAA Conformer							EEE Conformer		
	Theoretical AAE					α-solid			Theoretical AAA					Vapor	β-solid	Theoretical EEE		
	MP2/6-31G		B3LYP/6-311+G**			Ref. [9]	Ref. [21]		MP2/6-31		B3LYP/6-311+G**			Ref. [9]	Ref. [9]	B3LYP/6-311+G**		
υ	Freq.	Int.	Freq.	Int.	Irr. Rep.	IR	IR	Raman	Freq.	Int.	Freq.	Int.	Irr. Rep.	IR	IR	Freq.	Int.	Irr. Rep.
18	1,365	543	1,337	530	A	1,268 s	1,275 vs	1,273 s	1,371	351	1,345	1,034	A_1	1,319 s	1,313 s	1,334	91	E
19	1,322	1156	1,299	468	A′				1,316	115	1,294	546	E	1,268 s	1,261 s	1,297	205	E
20	1,320	219	1,296	107	A				1,316	115	1,292	534	E			1,295	267	E
21	1,305	79	1,270	28	A′	1,234 m	1,234 m	1,232 sh	1,309	0	1,275	11	A_2	1,218 w,b	1,218 b	1,274	167	E
22	1,294	218	1,264	339	A	1,218 m	1,219 m	1,214 s	1,282	96	1,252	208	E			1,274	163	E
23	1,272	198	1,238	112	A′	1,181 w			1,281	96	1,250	202	E			1,248	21	E
24	1,246	49	1,230	87	A	1,143 w			1,258	7	1,242	84	A_1			1,245	1	E
25	1,195	0	1,153	8	A′	1,039 s	1,040 s	1,029 w	1,184	0	1,141	0	A_2		1,142 w	1,180	0	A_2
26	1,069	107	1,036	141	A′	1,019 w	1,019 m		1,032	39	1,005	192	E	1,014 w,b	1,018 w,b	1,061	426	E
27	1,040	529	1,011	588	A	947 m	947 m	943 w	1,032	39	1,005	209	E			1,059	416	E
28	979	677	951	723	A	925 s	926 s	~920 w	952	180	935	574	A_1		931 m	993	38	A_1
29	967	429	937	922	A	915 s	915 sh		937	184	907	1,374	E	910 s	904 s	990	147	E
30	954	689	909	120	A′	883 m	883 m	884 vs	937	184	906	1,364	E			989	149	E
31	912	113	896	235	A	853 w	853 w	855 sh	908	1	887	113	A_1	880 m	877 m	910	209	A_1
32	864	477	870	53	A′	844 w	844 w	847 s	856	24	864	3	E	845 w	845 w	888	126	E
33	859	113	855	175	A	782 m	783 s	786 w	856	24	863	1	E			888	125	E
34	803	321	803	292	A		755 m	756 vw	783	116	782	471	A_1	782 m	774 m	819	25	A_1

Notes: vs - very strong, s - strong, m - medium, b - broad, sh - shoulder.
Frequencies and corresponding IR intensities are in cm^{-1} and esu^2-cm^2, respectively.
Symmetry assignments correspond to the B3LYP/6-311+G** results only.

Table 3. Theoretical and Experimental Vibrational Frequencies of RDX Conformers (continued)

	AAE Conformer								AAA Conformer							EEE Conformer		
	Theoretical AAE					α-solid			Theoretical AAA					Vapor	β-solid	Theoretical EEE		
	MP2/6-31G		B3LYP/6-311+G**			Ref. [9]	Ref. [21]		MP2/6-31		B3LYP/6-311+G**			Ref. [9]	Ref. [9]	B3LYP/6-311+G**		
υ	Freq.	Int.	Freq.	Int.	Irr. Rep.	IR	IR	Raman	Freq.	Int.	Freq.	Int.	Irr. Rep.	IR	IR	Freq.	Int.	Irr. Rep.
35	766	29	769	18	A				748	3	754	0	E			763	25	E
36	756	16	761	0	A′				748	3	753	0	E			762	43	A_1
37	740	9	756	21	A	739 m	738 vw	739 vw	727	3	749	6	A_1			761	26	E
38	675	35	676	34	A		670 vw	669 w	668	4	661	33	E			701	3	E
39	657	0	651	4	A′		602 m	605 m	668	4	660	33	E			701	3	E
40	618	67	610	95	A		588 m	589 m	590	9	593	0	A_2			666	0	A_2
41	592	36	588	3	A′				592	9	590	74	E			589	64	E
42	577	19	579	70	A′		486 w	486 w,sh	592	0	590	71	E			588	64	E
43	512	172	463	22	A		461 w	463 m	506	27	458	246	A_1			362	6	E
44	482	77	438	54	A		410 w	414 m	484	5	442	59	A_1			361	6	E
45	434	1	406	84	A				441	1	413	9	E			350	0	A_2
46	432	64	403	6	A′				441	1	409	9	E			331	9	A_1
47	398	0	371	1	A′		345 vw	347 w	388	0	365	3	E			329	111	A_1
48	336	19	325	31	A				388	0	363	3	E			235	149	E
49	293	0	290	0	A′		223 vw	224 vs	292	0	301	0	A_2			232	149	E
50	250	37	229	31	A		208 vw	205 m	232	3	221	96	E			167	26	E
51	217	112	209	15	A′		104	106	232	3	220	94	E			164	31	E

Notes: vs - very strong, s - strong, m - medium, b - broad, sh - shoulder.
Frequencies and corresponding IR intensities are in cm^{-1} and esu^2-cm^2, respectively.
Symmetry assignments correspond to the B3LYP/6-311+G** results only.

Table 3. Theoretical and Experimental Vibrational Frequencies of RDX Conformers (continued)

	AAE Conformer								AAA Conformer							EEE Conformer		
	Theoretical AAE					α-solid			Theoretical AAA					Vapor	β-solid	Theoretical EEE		
	MP2/6-31G		B3LYP/6-311+G**			Ref. [9]	Ref. [21]		MP2/6-31		B3LYP/6-311+G**			Ref. [9]	Ref. [9]	B3LYP/6-311+G**		
υ	Freq.	Int.	Freq.	Int.	Irr. Rep.	IR	IR	Raman	Freq.	Int.	Freq.	Int.	Irr. Rep.	IR	IR	Freq.	Int.	Irr. Rep.
52	137	3	107	0	A			90	132	0	102	58	E			115	28	E
53	86	11	93	10	A′				131	0	100	0	E			114	24	E
54	67	0	74	1	A′				102	0	67	5	A_1			81	0	A_2
55	65	72	63	18	A				36	0	63	8	A_2			62	781	A_1
56	60	111	60	11	A				32	0	37		E			54	46	E
57	37	2	44	2	A′				32	0	31		E			52	44	E

Notes: vs - very strong, s - strong, m - medium, b - broad, sh - shoulder.
Frequencies and corresponding IR intensities are in cm^{-1} and esu^2-cm^2, respectively.
Symmetry assignments correspond to the B3LYP/6-311+G** results only.

Table 4. Theoretical Vibrational Frequencies (cm^{-1}) and Assignments of RDX Conformers

	AAE Conformer		AAA Conformer		EEE Conformer	
ν	Freq.	Assignment	Freq.	Assignment	Freq.	Assignment
1	3,206	CH st (eq)	3,194	CH st (eq)	3,203	CH st (eq)
2	3,205	CH st (eq)	3,192	CH st (eq)	3,200	CH st (eq)
3	3,199	HCH st	3,192	CH st (eq)	3,199	CH st (eq)
4	3,081	HCH st	3,070	CH st (ax)	2,964	CH st (ax)
5	3,016	CH st (ax)	3,064	CH st (ax)	2,959	CH st (ax)
6	3,015	CH st (ax)	3,064	CH st (ax)	2,958	CH st (ax)
7	1,668	O->N->O st (ax)	1,658	O->N->O st	1,637	O->N->O st
8	1,648	O->N->O st (ax)	1,658	O->N->O st	1,637	O->N->O st
9	1,623	O->N->O st (eq)	1,627	O->N->O st	1,619	O->N->O st
10	1,496	CH_2 sci	1,482	CH_2 rock	1,522	CH_2 sci
11	1,480	CH_2 sci	1,466	CH_2 rock	1,510	CH_2 sci
12	1,468	CH_2 sci	1,464	CH_2 rock	1,509	CH_2 sci
13	1,420	CH_2 wag	1,403	CH_2 wag	1,431	CH_2 wag
14	1,406	CH_2 wag	1,402	CH_2 wag	1,430	CH_2 wag
15	1,374	CH_2 tw	1,384	CH_2 tw	1,366	CH_2 wag
16	1,362	CH_2 wag	1,381	CH_2 tw	1,350	N-N st + O<-N->O st
17	1,362	CH_2 tw and N-N st	1,363	CH_2 wag	1,336	CH_2 tw + N-N st

Notes: Evaluated at the B3LYP/6-311+G* level.
st = stretch, b = bend, tw = twist, umb = umbrella, rot = rotation, sci = scissor.
The most prominent contribution to each mode is listed first.

Table 4. Theoretical Vibrational Frequencies (cm^{-1}) and Assignments of RDX Conformers (continued)

	AAE Conformer		AAA Conformer		EEE Conformer	
ν	Freq.	Assignment	Freq.	Assignment	Freq.	Assignment
18	1,337	CH_2 tw and N-N st (ax)	1,345	N-NO_2 umb + CH_2 rock	1,334	CH_2 tw + N-N st
19	1,299	N-N st (ax)	1,294	N-NO_2 umb + CH_2 wag	1,297	C-N st
20	1,296	N-N st (ax) + ONO st + HCH wag	1,292	N-NO_2 umb + CH_2 wag	1,295	C-N st
21	1,270	CH_2 tw	1,275	CH_2 tw	1,274	N-N st + NO_2 st + CH b (ax)
22	1,264	N-C st	1,252	C-N st + CH_2 sci	1,274	N-N st + NO_2 st + CH b (ax)
23	1,238	N-C st	1,250	C-N st + CH_2 sci	1,248	CH_2 rock
24	1,230	CH_2 rock	1,242	CH_2 rock + sci + ring b	1,245	CH_2 tw + C-N st
25	1,153	N-C st	1,141	C-N st	1,180	CH_2 tw + C-N st
26	1,036	CH_2 rock + CH_2 tw	1,005	Ring tw	1,061	CH_2 rock + CH_2 tw
27	1,011	N-N st (eq) + CH_2 tw + CH_2 rock	1,005	CH_2 rock + CH_2 tw + CH_2 sci	1,059	CH_2 rock + CH_2 tw
28	951	CH_2 rock + N-N (eq) st	935	Ring breathing+ CH_2 sci+O<-N->O st	993	CH_2 rock + N-N st
29	937	Ring-breathing	907	CH_2 sci + C-N st	990	CH_2 rock + C-N st + N-N st
30	909	C-N st + CH_2 rock + N-N st	906	CH_2 sci + C-N st	989	CH_2 rock + C-N st + N-N st
31	896	C-N st + N-N st (ax)	887	C-N st + O<-N->O st	910	Ring breathing
32	870	N-N st + NO_2 sci (ax)	864	C-N st + O<-N->O st	888	Ring breathing
33	855	C-N st + NO_2 sci(eq)	863	C-N st + O<-N->O st	888	Ring breathing
34	803	Ring b + NO_2 sci	782	N-N st + O<-N->O st + C-N st	819	Ring b

Notes: Evaluated at the B3LYP/6-311+G* level.
st = stretch, b = bend, tw = twist, umb = umbrella, rot = rotation, sci = scissor.
The most prominent contribution to each mode is listed first.

Table 4. Theoretical Vibrational Frequencies (cm^{-1}) and Assignments of RDX Conformers (continued)

	AAE Conformer		AAA Conformer		EEE Conformer	
ν	Freq.	Assignment	Freq.	Assignment	Freq.	Assignment
35	769	N-NO_2 umb (eq)	754	N-N st + O<-N->O st + C-N st	763	N-NO_2 umb
36	761	N-NO_2 umb (ax)	753	N-NO_2 umb	762	N-NO_2 umb
37	756	N-NO_2 umb (ax)	749	N-N st + NO_2 sci	761	N-NO_2 umb
38	676	Ring b	661	Ring st	701	CNC b + N-N st + ONO sci
39	651	Ring rock (NO_2's stationary)	660	Ring st	701	CNC b + N-N st + ONO sci
40	610	Ring b	593	Ring rot + C-N st	666	Ring rot + NO_2 rock
41	588	Ring tw	590	Ring tw	589	NO_2 rock
42	579	Ring tw + NO_2 rock (eq)	590	Ring tw	588	NO_2 rock
43	463	Ring b (folding) + N-N st (ax)	458	Ring breathing	362	Ring st
44	438	Ring b (folding)	442	Ring breathing, only C atoms	361	Ring st
45	406	Ring b (flattening)	413	Ring b	350	Ring rot + NO_2 rock
46	403	N-NC2 umb (ax. Carbons)	409	Ring b	331	Ring b
47	371	Ring tw	365	Ring st	329	Ring b + N-N st
48	325	Molecular St	363	Ring st	235	Ring tw
49	290	Ring rot	301	Ring rot + NO_2 rock	232	Ring tw
50	229	N-NC2 Umb (eq)	221	Molecular b + N-N st + NO_2 wag	167	Ring tw + NO_2 rock
51	209	Molecular b	220	Molecular b + N-N st + NO_2 wag	164	Ring tw + NO_2 rock

Notes: Evaluated at the B3LYP/6-311+G* level.
st = stretch, b = bend, tw = twist, umb = umbrella, rot = rotation, sci = scissor.
The most prominent contribution to each mode is listed first.

Table 4. Theoretical Vibrational Frequencies (cm^{-1}) and Assignments of RDX Conformers (continued)

	AAE Conformer		AAA Conformer		EEE Conformer	
ν	Freq.	Assignment	Freq.	Assignment	Freq.	Assignment
52	107	NO_2 rot (ax) + Molecular b	102	NO_2 rot + NO_2 rock + NO_2 wag	115	N-NO_2 rot + ring rock
53	93	NO_2 rot (eq)	100	NO_2 rot + NO_2 rock + NO_2 wag	114	N-NO_2 rot + ring rock
54	74	NO_2 rot (all)	67	Molecular st (NO_2 up, ring down)	81	N-NO_2 rot
55	63	NO_2 wag (ax)	63	NO_2 rock	62	NO_2 wag
56	60	NO_2 wag (eq)	37	Molecular b + NO_2 wag and rock	54	NO_2 wag
57	44	NO_2 wag (ax)	31	Molecular b + NO_2 wag and rock	52	NO_2 wag

Notes: Evaluated at the B3LYP/6-311+G* level.
st = stretch, b = bend, tw = twist, umb = umbrella, rot = rotation, sci = scissor.
The most prominent contribution to each mode is listed first.

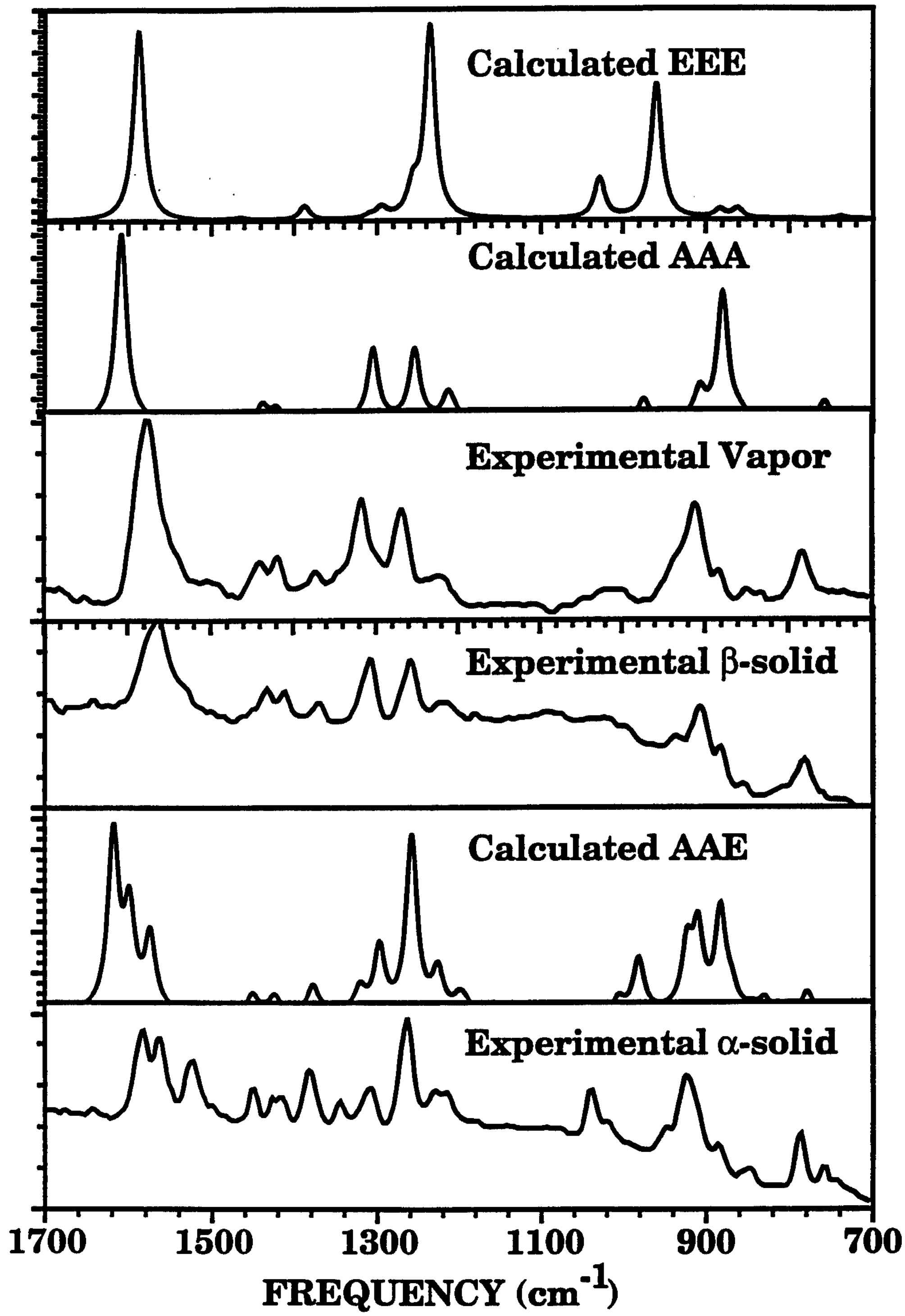

Figure 2. Simulated IR Spectra at the B3LYP/6-311+G** Level of the AAA, EEE, and AAE Conformers. The Vibrational Frequencies Used to Generate These Spectra Are Reduced by 3%. Experimental Spectra From Karpowicz and Brill [9] for α-RDX, β-RDX, and Vapor-Phase RDX Are Given for Comparison.

experimental spectra. These spectra offer strong support for the conclusions of the electron diffraction study that the AAA conformer is the most probable structure of RDX in the vapor phase [10]. These spectra also show that theoretical treatments are useful in differentiating between two possible conformers in the absence of diffraction data. We have also provided a comparison of our simulated AAE IR spectrum (frequencies reduced by 3%) with the experimental spectrum for the α-solid form in Figure 2. With the exception of the bands around 1,040 cm^{-1} in the experimental spectrum, most of the remaining experimental bands can be clearly assigned to a theoretical counterpart. This agreement between theory and experiment seems remarkably good, considering that the experimental spectrum includes effects of the crystal field, as well as overtones and combination bands.

Figure 3 provides a comparison of simulated IR spectra (using unscaled frequencies) for the three conformers at the B3LYP level using the 6-31G* and 6-311+G** basis sets. Figure 3 also includes spectra using MP2/6-31G* results for the AAE and AAA conformers. It is apparent that the features in the B3LYP spectra are relatively insensitive to basis sets. One of the prominent discrepancies between the two basis sets can be seen in all three conformers. This is the shift in the band reported in the 1,700–1,800 cm^{-1} range at the double-zeta (DZ) level to the lower-energy 1,600–1,700-cm^{-1} range for the triple-zeta (TZ) basis. A second prominent feature is evident in the AAE spectra and is seen in the relative intensities of the two bands at 1,337 and 1,362 cm^{-1} from the TZ basis set. These bands can mix since both are of A symmetry, and the 6-311+G** intensity of each band is 530 and 172 esu^2-cm^2, respectively. This ordering agrees with experiment (see Figure 2). The relative locations of these bands appear to be reversed at the DZ level. It is apparent that the MP2/6-31G* spectrum for the AAE conformer is substantially different from both B3LYP spectra. The MP2/6-31G* prediction of the spectrum of the AAA conformer also has features that differ from the B3LYP predictions, although not as pronounced as for the AAE comparison.

Absolute, relative, and zero-point energies of each conformer are given in Table 5. The B3LYP predictions using both 6-31G* and 6-311+G** basis sets indicate that the AAE conformer has the lowest energy of the three conformers, but only by a fraction of a kcal/mol. Similarly, the MP2/6-31G* predictions indicate that the AAE conformer is only slightly lower in energy than the

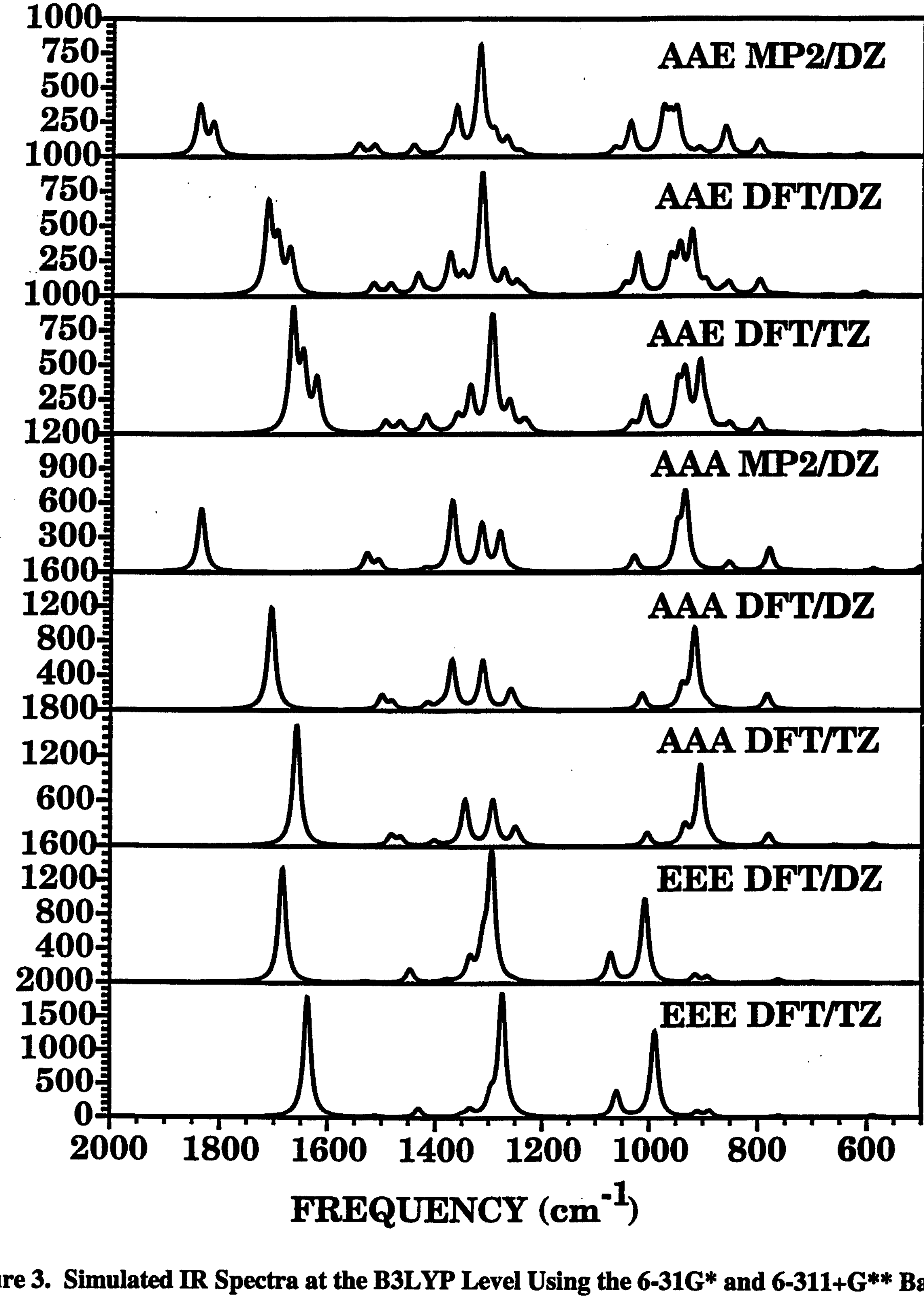

Figure 3. Simulated IR Spectra at the B3LYP Level Using the 6-31G* and 6-311+G** Basis Sets for the AAA, EEE, and AAE Conformers. MP2/6-31G* Spectra Are Also Included. Unscaled Vibrational Frequencies Were Used to Generate These Spectra. DZ Denotes the 6-31G* Basis Set, and TZ Denotes the 6-311+G** Basis Set.

Table 5. Absolute and Relative Energies of RDX Conformers

	MP2/6-31G*			B3LYP/6-31G*			B3LYP/6-311+G**		
	Absolute Energy (Hartrees)	Zero Point Energy (kcal/mol)	Relative[a] Energy (kcal/mol)	Absolute Energy (Hartrees)	Zero Point Energy (kcal/mol)	Relative[a] Energy (kcal/mol)	Absolute Energy (Hartrees)	Zero Point Energy (kcal/mol)	Relative[a] Energy (kcal/mol)
AAE	−895.0074868	91.76	0.0	−897.409356284	90.06	0.0	−897.679561669	89.11	0.0
AAA	−895.0070845	91.64	0.13	−897.408901632	89.95	0.18	−897.678331096	88.98	0.64
EEE				−897.400693145	89.59	4.97	−897.671751763	88.78	4.57

[a] Zero-point-corrected energies relative to AAE conformer.

AAA conformer (by 0.13 kcal/mol). The zero-point-corrected B3LYP/ 6-31G* and B3LYP/ 6-311+G** energies of the AAA conformer are 0.18 and 0.64 kcal/mol, respectively, relative to AAE. Within the level of accuracy for the calculations, the AAE and AAA conformers are identical in their stability. The B3LYP/6-31G* and B3LYP/6-311+G** zero-point-corrected energies of the EEE conformer are 4.97 and 4.57 kcal/mol, respectively, relative to AAE. The earlier SCF/4-21G calculations had the energy ordering reversed for the AAE and AAA conformers [7]. In that study, the AAA was more stable by 0.6 kcal/mol [7]. Also, the EEE was less stable than AAA by 7.2 kcal/mol [7]. Karpowicz and Brill suggest that the intermolecular forces of neighboring RDX molecules in the α-RDX crystal are responsible for "the energetically unlikely positioning of the NO_2 groups that produces approximately C_s molecular symmetry" [9]. The calculations presented here suggest that the positioning of the NO_2 groups in the AAE conformer is not "energetically unlikely."

3. Conclusions

Three conformers of the large polyatomic explosive RDX have been located, and their structures and vibrational spectra characterized with nonlocal DFT treatments using DZ and TZ quality basis sets. The three conformers have the NO_2 oriented in either AAE, AAA, and EEE arrangements relative to the ring. The AAA structure is consistent with electron diffraction results of vapor-phase RDX [10], and the AAE conformer is consistent with that of the room-temperature-stable RDX crystal [8]. Additionally, the AAA and AAE conformers are calculated using MP2 theory for comparison with the DFT predictions. Of the three levels of theoretical treatment, the B3LYP/6-311+G** predictions of the geometry of the AAE conformer are in closest overall agreement with experiment, and MP2/6-31G* predictions are in the poorest overall agreement with experiment. The B3LYP/6-311+G** results for the AAE conformer are in agreement with experiment to within 2% for all bond lengths with the exception of a single C-H bond (3.7%) and the N-N bonds (2.5–4.0%). The B3LYP/6-311+G** predictions of bond angles are within 1.6% of experiment with the exception of two C-N-N angles (3.6–4.5%). In general, the B3LYP/6-311+G** level produces the closest overall agreement with all available experimental data for structures and spectra.

Structural parameters for the AAA conformer are in closer agreement to experiment [10] than those predicted for the EEE conformer. Additionally, simulated IR vibrational spectra of the AAA conformer compare well with experimental spectra of vapor-phase and β-solid RDX, while the simulated spectrum of the EEE conformer did not. The differences in predicted geometries and vibrational spectra between the AAA and EEE conformers support the experimental conclusions that RDX in the vapor- and β-solid phases have C_{3v} symmetry [9] and have the nitro groups arranged in the AAA configuration [10]. In addition to providing atomic-level information about a well-studied explosive, the results presented here provide another indication that DFT methods can be applied to large polyatomic molecules with a small computational cost and reliable results for molecular structure, intramolecular force fields, and vibrational spectra.

4. References

1. Hohenberg, P., and W. Kohn. *Phys. Rev. B.* Vol. 136, p. 864, 1964.

2. Kohn, W., and L. J. Sham. *Phys. Rev. A.* Vol. 140, p. 113, 1965.

3. Zeigler, T. *Chem. Rev.* Vol. 91, p. 651 (and references therein), 1991.

4. Labanowski, J., and J. Andzelm (eds.). *Density Functional Methods in Chemistry.* Springer: Berlin, 1991.

5. Politzer, P., J. M. Seminario (eds.). *Theoretical and Computational Chemistry.* Elsevier Scientific: Amsterdam, vol. 1, 1995.

6. Habibollahzadeh, D., M. Grodzicki, J. M. Seminario, and P. Politzer. *J. Phys. Chem.* Vol. 95, p. 7699, 1991.

7. Coffin, J. M., S. Q. Newton, J. D. Ewbank, L. Schäfer, C. Van Alsenoy, and K. Siam. *J. Mol. Struct. (THEOCHEM).* Vol. 251, p. 219, 1991.

8. Choi, C. S., and E. Prince. *Acta. Crystallogr. Sect. B.* Vol. 28, p. 57, 1972.

9. Karpowicz, R. J., and T. B. Brill. *J. Phys. Chem.* Vol. 88, p. 348, 1984.

10. Shishkov, I. F., L. V. Vilkov, M. Kolonits, and B. Rozsondai. *Struct. Chem.* Vol. 2, p. 57, 1991.

11. Moeller, C., and M. S. Plesset. *Phys. Rev.* Vol. 46, p. 618, 1934.

12. Hehre, W. J., R. Ditchfield, and J. A. Pople. *J. Chem. Phys.* Vol. 56, p. 2257, 1972.

13. Hariharan, P. C., and J. A. Pople. *Theor. Chim. Acta.* Vol. 28, p. 213, 1973.

14. Gordon, M. S. *Chem. Phys. Lett.* Vol. 76, p. 163, 1980.

15. McLean, A. D., and G. S. Chandler. *J. Chem. Phys.* Vol. 72, p. 5639, 1980.

16. Krishnan, R., J. S. Binkley, R. Seeger, and J. A. Pople. *J. Chem. Phys.* Vol. 72, p. 650, 1980.

17. Becke, A. D. *Phys. Rev. A.* Vol. 38, p. 3098, 1988.

18. Lee, C., W. Yang, and R. G. Parr. *Phys. Rev. B.* Vol. 37, p. 785, 1988.

19. Meihlich, G., A. Savin, H. Stoll, and H. Preuss. *Chem. Phys. Lett.* Vol. 157, p. 200, 1989.

20. Frisch, M. J., G. W. Trucks, H. B. Schlegel, P. M. W. Gill, B. G. Johnson, M. A. Robb, J. R. Cheeseman, T. Keith, G. A. Petersson, J. A. Montgomery, K. Raghavachari, M. A. Al-Laham, V. G. Zakrzewski, J. V. Ortiz, J. B. Foresman, J. Cioslowski, B. B. Stefanov, A. Nanayakkara, M. Challacombe, C. Y. Peng, P. Y. Ayala, W. Chen, M. W. Wong, J. L. Andres, E. S. Replogle, R. Gomperts, R. L. Martin, D. J. Fox, J. S. Binkley, D. J. Defrees, J. Baker, J. P. Stewart, M. Head-Gordon, C. Gonzalez, and J. A. Pople. *Gaussian 94.* Revision B.1, Gaussian, Inc., Pittsburgh, PA, 1995.

21. Rey-Lafon, M., C. Trinquecoste, R. Cavagnat, and M.-T. Forel. *J. Chim. Phys. Chem. Biol.* Vol. 68, p. 1533, 1971.

NO. OF COPIES	ORGANIZATION
2	DEFENSE TECHNICAL INFORMATION CENTER DTIC DDA 8725 JOHN J KINGMAN RD STE 0944 FT BELVOIR VA 22060-6218
1	HQDA DAMO FDQ DENNIS SCHMIDT 400 ARMY PENTAGON WASHINGTON DC 20310-0460
1	DPTY ASSIST SCY FOR R&T SARD TT F MILTON RM 3EA79 THE PENTAGON WASHINGTON DC 20310-0103
1	OSD OUSD(A&T)/ODDDR&E(R) J LUPO THE PENTAGON WASHINGTON DC 20301-7100
1	CECOM SP & TRRSTRL COMMCTN DIV AMSEL RD ST MC M H SOICHER FT MONMOUTH NJ 07703-5203
1	PRIN DPTY FOR TCHNLGY HQ US ARMY MATCOM AMCDCG T M FISETTE 5001 EISENHOWER AVE ALEXANDRIA VA 22333-0001
1	PRIN DPTY FOR ACQUSTN HQS US ARMY MATCOM AMCDCG A D ADAMS 5001 EISENHOWER AVE ALEXANDRIA VA 22333-0001
1	DPTY CG FOR RDE HQS US ARMY MATCOM AMCRD BG BEAUCHAMP 5001 EISENHOWER AVE ALEXANDRIA VA 22333-0001

NO. OF COPIES	ORGANIZATION
1	INST FOR ADVNCD TCHNLGY THE UNIV OF TEXAS AT AUSTIN PO BOX 202797 AUSTIN TX 78720-2797
1	USAASA MOAS AI W PARRON 9325 GUNSTON RD STE N319 FT BELVOIR VA 22060-5582
1	CECOM PM GPS COL S YOUNG FT MONMOUTH NJ 07703
1	GPS JOINT PROG OFC DIR COL J CLAY 2435 VELA WAY STE 1613 LOS ANGELES AFB CA 90245-5500
1	ELECTRONIC SYS DIV DIR CECOM RDEC J NIEMELA FT MONMOUTH NJ 07703
3	DARPA L STOTTS J PENNELLA B KASPAR 3701 N FAIRFAX DR ARLINGTON VA 22203-1714
1	USAF SMC/CED DMA/JPO M ISON 2435 VELA WAY STE 1613 LOS ANGELES AFB CA 90245-5500
1	US MILITARY ACADEMY MATH SCI CTR OF EXCELLENCE DEPT OF MATHEMATICAL SCI MDN A MAJ DON ENGEN THAYER HALL WEST POINT NY 10996-1786
1	DIRECTOR US ARMY RESEARCH LAB AMSRL CS AL TP 2800 POWDER MILL RD ADELPHI MD 20783-1145

NO. OF COPIES	ORGANIZATION
1	DIRECTOR US ARMY RESEARCH LAB AMSRL CS AL TA 2800 POWDER MILL RD ADELPHI MD 20783-1145
3	DIRECTOR US ARMY RESEARCH LAB AMSRL CI LL 2800 POWDER MILL RD ADELPHI MD 20783-1145
	ABERDEEN PROVING GROUND
4	DIR USARL AMSRL CI LP (305)

REPORT DOCUMENTATION PAGE

Form Approved OMB No. 0704-0188

1. AGENCY USE ONLY *(Leave blank)*

2. REPORT DATE
January 1998

3. REPORT TYPE AND DATES COVERED
Final, Jan - Dec 96

4. TITLE AND SUBTITLE
Ab Initio and Nonlocal Density Functional Study of 1,3,5-trinitro-s-triazine (RDX) Conformers

5. FUNDING NUMBERS
1L161102AH43

6. AUTHOR(S)
Betsy M. Rice and Cary F. Chabalowski

7. PERFORMING ORGANIZATION NAME(S) AND ADDRESS(ES)
U.S. Army Research Laboratory
ATTN: AMSRL-WM-PC
Aberdeen Proving Ground, MD 21005-5066

8. PERFORMING ORGANIZATION REPORT NUMBER
ARL-TR-1586

9. SPONSORING/MONITORING AGENCY NAMES(S) AND ADDRESS(ES)

10. SPONSORING/MONITORING AGENCY REPORT NUMBER

11. SUPPLEMENTARY NOTES

12a. DISTRIBUTION/AVAILABILITY STATEMENT
Approved for public release; distribution is unlimited.

12b. DISTRIBUTION CODE

13. ABSTRACT *(Maximum 200 words)*

Geometry optimizations and normal-mode analyses of three conformers of 1,3,5-trinitro-s-triazine (RDX) are performed using second-order Moller-Plesset (MP2) and nonlocal density functional theory (DFT) methods. The density function used in this study is B3LYP. The three conformers of RDX are distinguished mainly by the arrangement of the nitro groups relative to the ring atoms of the RDX molecule. NO_2 groups arranged in either pseudo-equatorial or axial positions are denoted with (E) or (A), respectively. The axial-axial-equitorial (AAE) conformer has C_s symmetry and is the structure in the room-temperature-stable crystal (α-RDX). The axial-axial-axial (AAA) and equitorial-equitorial-equitorial (EEE) conformers have C_{3v} symmetry, a symmetry consistent with vapor and β-solid infrared (IR) spectra. The AAE and AAA conformers are studied at the MP2/6-31G*, B3LYP/6-31G*, and B3LYP/6-311+G** levels, and the EEE conformer is studied using the B3LYP density function and the 6-31G* and 6-311+G** basis sets. The geometric parameters and IR spectra of the AAA conformer are in good agreement with experimental gas-phase and β-solid data, supporting the hypotheses derived from experiment that the AAA structure is the most probable conformer in vapor-phase and β-solid RDX. The B3LYP/ 6-311+G** structures and simulated IR spectra are in closest agreement with experimental data. The MP2/6-31G* structures and spectra are in poorest agreement with experiment.

14. SUBJECT TERMS
RDX, *ab initio*, density functional theory, 1,3,5-trinitro-s-triazine, vibrational spectra

15. NUMBER OF PAGES
36

16. PRICE CODE

17. SECURITY CLASSIFICATION OF REPORT	18. SECURITY CLASSIFICATION OF THIS PAGE	19. SECURITY CLASSIFICATION OF ABSTRACT	20. LIMITATION OF ABSTRACT
UNCLASSIFIED	UNCLASSIFIED	UNCLASSIFIED	UL

NSN 7540-01-280-5500

Standard Form 298 (Rev. 2-89)
Prescribed by ANSI Std. 239-18 298-102

INTENTIONALLY LEFT BLANK.

USER EVALUATION SHEET/CHANGE OF ADDRESS

This Laboratory undertakes a continuing effort to improve the quality of the reports it publishes. Your comments/answers to the items/questions below will aid us in our efforts.

1. ARL Report Number/Author ARL-TR-1586 (Rice) ____________ Date of Report January 1998 ________

2. Date Report Received ____

3. Does this report satisfy a need? (Comment on purpose, related project, or other area of interest for which the report will be used.) ____

____

____

4. Specifically, how is the report being used? (Information source, design data, procedure, source of ideas, etc.) ________

____

____

5. Has the information in this report led to any quantitative savings as far as man-hours or dollars saved, operating costs avoided, or efficiencies achieved, etc? If so, please elaborate. ____

____

____

6. General Comments. What do you think should be changed to improve future reports? (Indicate changes to organization, technical content, format, etc.) ____

____

____

____

CURRENT ADDRESS

____
Organization

____
Name | E-mail Name

____
Street or P.O. Box No.

____
City, State, Zip Code

7. If indicating a Change of Address or Address Correction, please provide the Current or Correct address above and the Old or Incorrect address below.

OLD ADDRESS

____
Organization

____
Name

____
Street or P.O. Box No.

____
City, State, Zip Code

(Remove this sheet, fold as indicated, tape closed, and mail.)

(DO NOT STAPLE)

DEPARTMENT OF THE ARMY

OFFICIAL BUSINESS

NO POSTAGE
NECESSARY
IF MAILED
IN THE
UNITED STATES

BUSINESS REPLY MAIL
FIRST CLASS PERMIT NO 0001,APG,MD

POSTAGE WILL BE PAID BY ADDRESSEE

DIRECTOR
US ARMY RESEARCH LABORATORY
ATTN AMSRL WM PC
ABERDEEN PROVING GROUND MD 21005-5066